Eur J Nucl Med Mol Imaging (2008) 35:264–271
DOI 10.1007/s00259-007-0576-1

ORIGINAL ARTICLE

# PET/CT with Gluc-Lys-([$^{18}$F]FP)-TOCA: correlation between uptake, size and arterial perfusion in somatostatin receptor positive lesions

**Hinrich Wieder · Ambros J. Beer · Thorsten Poethko · Guenther Meisetschlaeger · Hans-Juergen Wester · Ernst Rummeny · Markus Schwaiger · Alexander R. Stahl**

Received: 23 May 2007 / Accepted: 27 August 2007 / Published online: 3 October 2007


**Abstract**
*Purpose* Somatostatin receptor (sstr) positive tumours vary widely in uptake of radiolabelled somatostatin (sst) analogues. This study determinates variability in lesion uptake of the glycosylated sst analogon $N^{\alpha}$-(1-deoxy-D-fructosyl)-$N^{\varepsilon}$-(2-[$^{18}$F]fluoropropionyl)-Lys$^{0}$-Tyr$^{3}$-octreotate (Gluc-Lys([$^{18}$F]FP)-TOCA) and correlates it with lesion size and arterial perfusion as measured on computed tomography (CT).
*Methods* Ten patients with metastasized neuroendocrine carcinomas were investigated with positron emission tomography PET/CT (Biograph 16, Siemens, Germany). Lesion standardized uptake values (SUVs) were determined at ~50 min post tracer injection according to a 60% isocontour volume of interest around each lesion. Lesion size and enhancement in the arterial phase (hounsfield units, HUs) were derived from CT.
*Results* 114 lesions in the upper abdomen had a correlate on both, PET and CT. Variability in lesion SUVs was high ($SUV_{mean}$ 22±13). Intraindividually, there was a sigmoid positive correlation between lesion SUV and lesion diameter indicating partial volume effects. Residual variability in lesions ≥3 cm (≥2.5 cm) ranged down to about half (third) of the maximum lesion uptake and remained unexplained by partial volume effects. No correlation with measured HU in the arterial phase was found, neither intraindividually nor interindividually.
*Conclusion* Partial volume effects were a major source of intraindividual variability in tumour tracer uptake. Lesions below 2.5 to 3 cm should thus be used with caution when performing dose calculations. In larger lesions residual variability in uptake must be considered; it may be due to variable sstr2 expression on the tumours' cell surfaces.

**Keywords** Somatostatin receptor · Partial volume effect · Peptide receptor · Radionuclide therapy · Neuroendocrine carcinoma

H. Wieder · A. J. Beer · T. Poethko · G. Meisetschlaeger · H.-J. Wester · M. Schwaiger · A. R. Stahl (✉)
Department of Nuclear Medicine, Technische Universität München, Klinikum rechts der Isar,
Ismaninger Str. 22,
81675 Munich, Germany
e-mail: a.stahl@lrz.tum.de

H. Wieder · E. Rummeny
Department of Radiology, Technische Universität München,
Klinikum rechts der Isar,
Ismaninger Str. 22,
81675 Munich, Germany

A. R. Stahl
Department of Radiology, Universitätsklinikum Essen,
Hufelandstr. 55,
45147 Essen, Germany

## Introduction

Recently, the glycosylated $^{18}$F-labelled somatostatin analogue $N^{\alpha}$-(1-deoxy-D-fructosyl)-$N^{\varepsilon}$-(2-[$^{18}$F]fluoropropionyl)-Lys$^{0}$-Tyr$^{3}$-octreotate (Gluc-Lys([$^{18}$F]FP)-TOCA) has been introduced for somatostatin receptor (sstr)—PET [1–3]. Gluc-Lys([$^{18}$F]FP)-TOCA exhibits favourable pharmacokinetic characteristics such as high uptake in sstr-positive tumours, rather low lipophilicity, plasma protein binding and hepatic uptake, and rapid renal excretion. Excellent tumour/non-tumour ratios in tracer uptake are achieved as early as 30 min post

injection; the diagnostic yield in terms of detected tumour lesions is more than two times as high as with the standard imaging agent [$^{111}$In]DTPA-octreotide. Gluc-Lys([$^{18}$F]FP)-TOCA demonstrates a very high affinity to somatostatin receptor subtype 2 ($sstr_2$), which is the predominant subtype in sstr-positive tumours such as neuroendocrine carcinoma. Affinity to $sstr_2$ is by a factor ten higher than that of [$^{111}$In]DTPA-octreotide [3, 4].

A major pharmacokinetic difference between somatostatin analogues labelled with radiohalogenes such as Gluc-Lys([$^{18}$F]FP)-TOCA or [$^{123}$I]Mtr-TOCA [5, 6] and those with radiometals such as [$^{111}$In]DTPA-octreotide or [$^{68}$Ga-DOTA, Tyr3]octreotide [7] is the fate of the radiolabel after binding to the sstr, cellular internalization, and subsequent lysozymal degradation of the ligand–receptor complex. Whereas fragments labelled with radiometals are known to be trapped within cells, no such trapping has been found for those labelled with radiohalogenes [8]. Consequently, from 3 h on, a leakage of tumour activity has been observed for somatostatin analogues labelled with radiohalogenes [5]. Characteristically, tumour uptake of Gluc-Lys([$^{18}$F]FP)-TOCA reaches a plateau at 30–40 min post injection, which lasts for 2 h [1].

It is a daily experience in clinical routine imaging that sstr positive tumours vary widely in uptake of radiolabelled somatostatin analogues on a lesion-by-lesion and on a patient-by-patient basis. A better understanding of this variability would be important not only for diagnostic purposes, but even more for appropriate dosing of radiolabelled somatostatin analogues in peptide receptor radionuclide therapy [9–14]. However, to our knowledge, no systematic investigation of variability in tumour uptake of radiolabelled somatostatin analogues has been performed by now.

This PET/CT study investigates the variability in tumour uptake of Gluc-Lys([$^{18}$F]FP)-TOCA and correlates it with key parameters of morphological imaging, namely, lesion size and enhancement in the arterial phase in computed tomography (CT). In detail the questions addressed are:

- How much variability can be found in tumour tracer uptake, intraindividually and interindividually?
- How is the correlation between tracer uptake and tumour size?
- Is there any correlation between tracer uptake and enhancement in the arterial phase on CT?

## Materials and methods

### Patients

Ten patients (six male, four female; age 61.1±7.5 years, range 50–70 years) were investigated. Eight patients suffered from metastasized neuroendocrine carcinomas—of the intestine (five patients), the bronchial tree (one patient), the pancreas (one patient), and of unknown origin (one patient). One patient each suffered from malignant gastrinoma of the pancreas and from pheochromocytoma of the adrenal gland. All patients were off somatostatin analogues—at least 2 months after injection of long-acting agents and at least 3 days in case of short-acting ones. Written informed consent was obtained from all patients. The study was approved by the local ethics committee.

### Instrumentation

The patients were investigated with the PET/CT system Biograph 16 (Siemens, Forchheim, Germany). The Biograph 16 combines a 16-slice helical CT scanner and a PET scanner with a 16.2-cm axial field of view. The spatial resolution of the PET component is 5.9 and 5.5 mm, transaxially and axially, at 1 cm off the centre of the gantry (specification from the manufacturer according to the methodology of NEMA standard publication NU 2 2001).

### Imaging protocol

The radiopharmaceutical Gluc-Lys([$^{18}$F]FP)-TOCA was synthesized as described elsewhere [3]. Patients were injected with ~ 100 MBq Gluc-Lys([$^{18}$F]FP)-TOCA at ~50 min before PET imaging.

At first, a low-dose CT scan from the base of the skull to the bottom of the pelvis was acquired to perform transmission correction for the PET scan. The subsequent PET scan was acquired in 3D mode from the base of the skull to the bottom of the pelvis (5–8 bed positions, 2 min per bed position). Transversal PET slices were iteratively reconstructed with a thickness of 3 mm.

After PET, a diagnostic CT scan was performed (tube current 150 mAs, voltage 120 kV, collimation 16× 0.75 mm; reconstructed slice thickness/reconstruction increment: 3/3 mm). Scanning of the abdomen was performed in the arterial enhancement phase using bolus tracking. For this purpose, each patient was first injected with a test bolus of contrast medium and the appropriate time delay for imaging the arterial phase was calculated by using a region of interest (ROI) in the aortic arch. After that, patients were injected with the diagnostic amount of contrast medium. Scanning of the body from head to pelvis was performed in the portal-venous phase with a delay of 70 s p.i. Injection of 120 ml of contrast medium (Imeron 300, Altana, Konstanz, Germany) was performed at a rate of 3 ml/s. Patient preparation for CT consisted of oral administration of 1,000 ml of diluted contrast medium more than 1 h before imaging.

### Data analysis

PET analysis was based on placement of volumes of interest (VOIs) around each lesion and determination of standardized uptake values (SUVs) from these VOIs according to the equation

$$\mathrm{SUV} = \frac{\mathrm{activity}_{\mathrm{measured}} * \mathrm{bodyweight}[\mathrm{g}]}{\mathrm{activity}_{\mathrm{injected}} * \mathrm{volume}_{\mathrm{VOI}}[\mathrm{ml}]} \quad (1)$$

The outer border of each lesion VOI was semiautomatically defined by an isocontour representing 60% of the maximum activity within the VOI. Both $SUV_{mean}$ (mean value from all pixels included in VOI) and $SUV_{max}$ (i.e., maximum pixel value within VOI), were calculated from each lesion VOI. In addition, $SUV_{mean}$ and $SUV_{max}$ were determined for normal liver tissue by manually placing a round ~5 cm region of interest (without isocontour) into healthy liver. Tumor lesions outside the field of view of arterial phase CT were not considered, nor were bone lesions analysed as they are difficult to assess on CT in terms of size and HU. The primary tumour was not included in the analysis because it was either out of the field of arterial phase CT or already removed or unknown.

Each PET lesion was tried to spot on arterial phase CT. If no correlate was detectable the venous phase CT and overlay images from PET/CT were included. If still not identifiable, the lesion was not analysed on CT but marked as "PET only". Identifiable lesions were measured with respect to size (arterial phase CT or venous phase CT—wherever better visible) and to HU at the arterial phase. To measure HUs, a small ROI was manually placed within the lesion and the mean HU and the standard deviation were noted. In case of inhomogeneous density of a lesion, the ROI was placed in the respective maximum. In case of centrally cystic lesions, the ROI was placed in the (hyper-)perfused rim of the lesion. The measured lesion HUs ranged from ~80 to ~110. Overall, 5/114 lesions (see "Results") had a cystic centre, the centrally measured HUs of which (~0 to ~30) were not used for analysis. All analyses were done by a single investigator with 8 years experience in PET reading and 2 years experience in CT reading.

### Statistics

The Statistica software package was used (Statsoft, Germany) to produce fitted curves to two-dimensional data. The Statview software package (Statview, SAS Institute, Cary, NY)) was used to perform simple and multiple regression analysis. For data comparison a Mann–Whitney *U* test (unpaired data) or a Wilcoxon signed rank test (paired data) was used. All analyses were done on a 5% level for the statistical probability of a type I error (alpha).

## Results

In ten patients, a total of 144 lesions were observed in the upper abdomen on PET (leaving out bone lesions). Three of 144 lesions were initially overseen on PET and only retrospectively detected after review of the CT (one lymph node initially considered "statistical scatter"; one lymph node initially considered intestinal uptake; one lesion in the duodenum initially considered urinary accumulation). Eight of 144 lesions were reported as uncertain on PET. According to CT, four of these uncertain lesions turned out to be true lesions in the liver, whereas four lesions (two and two) turned out to be normal gall bladder and normal adrenal gland, respectively. Two of 144 lesions were considered a positive lymph node and a liver lesion on PET, respectively, but after review of the CT they turned out to be normal adrenal gland and a positive lymph node. Overall, a total of 139 true lesions were detected on PET with "true" meaning a presumable tumour lesion "not disproven" on CT or overlay PET/CT. One hundred eight lesions were located in the liver, 31 lesions were located outside the liver.

Of 139 true lesions on PET, 82 were readily seen on arterial phase CT (59%). Additional 16 lesions were detected on portal venous phase only; additional eight lesions were detected on superimposed PET/CT only. Of the remaining 33/139 lesions (24%) the identification of eight remained slightly uncertain, but was taken as almost clear on CT after complete revision of all phases of CT and with the aid of overlay images (one lesion in the pancreas, seven lymph nodes below 1 cm in transversal diameter). Overall, of 139 true lesions on PET, 114 (82%) were clearly or almost clearly spotted on CT. Five of these 114 lesions had a cystic centre.

Twenty-five of 139 lesions (18%) were not found at all on CT ("PET only" lesions, see Fig. 1). However, CT helped to clarify organ affiliation in three of these 25 lesions (one in the pancreas, two in an operated liver). Lesion characteristics ($n$= 114) in terms of lesion SUV, lesion size and measured HU on arterial phase CT are shown in Table 1. In addition, $SUV_{mean}$ and measured HU for normal liver tissue are presented.

### Intraindividual analysis

To adjust for interindividual differences, lesions were normalized for $SUV_{mean/max}$ and measured HU. For this purpose, the intraindividual lesion having the maximum respective value was set to 100% provided that this lesion was ≥2 cm to avoid major partial volume effects on PET.

Figure 2 plots normalized $SUV_{mean}$ against lesion size. There is a clear positive correlation between lesion size and

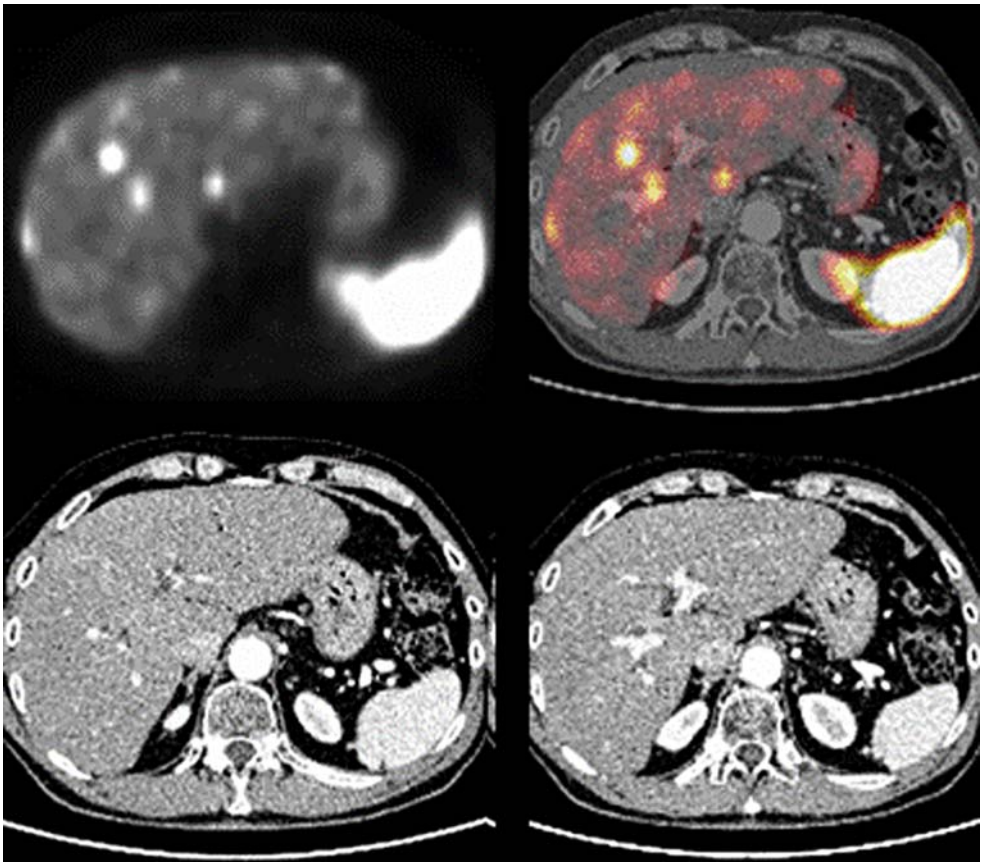

**Fig. 1** Clear visualization of liver metastases on PET (*upper left*) and overlay PET/CT (*upper right*) but no morphological correlate on arterial phase CT (*lower left*) and portal venous phase CT (*lower right*)

$SUV_{mean}$. The correlation can be fitted with a sigmoid curve of the form

$$SUV = 100\frac{a}{1+e^{-(\text{size}-b)/c}} + d, \quad (2)$$

where $b$ determines the shift on the $x$-axis, $c$ the slope of the curve, $d$ the shift on the $y$-axis and $a$ adjusts for a less than 100% interval of values on the $y$-axis. Best fitting was achieved for $SUV_{mean}$ (and also for $SUV_{max}$, data not shown in detail) with:

$$SUV = 100\frac{0.95}{1+e^{-(\text{size}-1.4)/0.4}} + 5 \quad (3)$$

Using this equation, the resulting sigmoid curve (Fig. 2) reaches its terminal plateau between a lesion size of 2.5 cm (calculated normalized SUV=94%) and 3 cm (98%). Note the measured SUVs for lesions between 2.5 (3 cm) and 4 cm varying considerably from ~30 to 100% (~50 to 100%) that is by a factor ~3 (~2). Detailed analysis of this subgroup revealed no physical explanation for a decrease in SUV such as an extraordinarily high-ratio lesion/background, which could have given rise to an extraordinarily high partial volume effect. Instead, even in the same patient and organ (i.e. liver), the SUVs in lesions from 2.5 to 4 cm varied from ~30 to 100%. There was no significant change to the diagrams when restricting the analysis to liver lesions only (data not shown). Table 2 opposes results from small lesions (<1 cm) to those from large lesions (>2.5 cm).

**Table 1** Overall variability observed in lesion SUV, size and HUs as well as liver SUV and HUs

| | Mean | Standard deviation |
|---|---|---|
| Lesion $SUV_{mean}$ | 21.7 | 13.0 |
| Lesion $SUV_{max}$ | 28.4 | 16.8 |
| Lesion $SUV_{mean}$ (≥2 cm, $n$=25) | 34.5 | 13.9 |
| Lesion size | 1.81 | 1.95 |
| Lesion HU | 98 | 20 |
| Liver SUV | 7.32 | 5.66 |
| Liver HU | 77 | 9.4 |

There was no relationship between lesion size and normalized HU (Fig. 3). For this reason, any size criteria for normalization of HU were abandoned. Normalized HU were calculated by simply setting the intraindividual lesion with the highest HU to 100%.

Figure 4 shows no overall relationship between normalized $SUV_{mean}$ and normalized HU. This was also true for $SUV_{max}$ or when restricting analysis to liver lesions only (data not shown). Figure 5 illustrates in a more detailed way the missing correlation between crude measured HU and crude measured SUV by only using lesions above 2.5 cm to avoid partial volume effects. No overall correlation was present, nor was there any significant trend/pattern in individual patients ($p$=0.31).

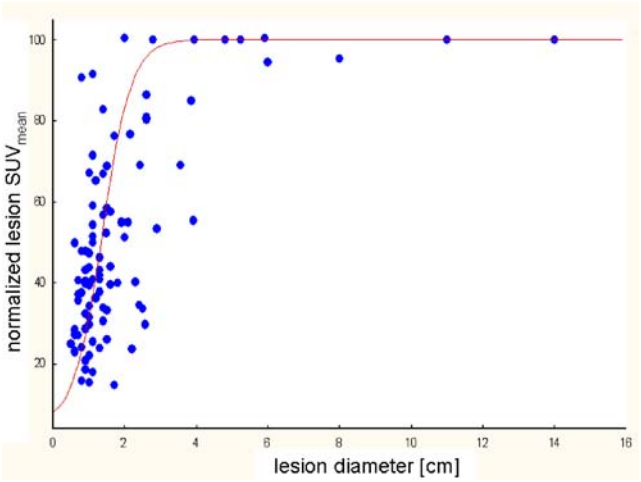


**Fig. 2** Sigmoid correlation of lesion size and lesion SUV after nivellation of interindividual differences in lesion SUVs by setting the intraindividual lesion with maximum $SUV_{mean}$ to 100% (precondition: lesion size ≥2 cm)

### Interindividual analysis

For interindividual analysis, the median measured $SUV_{mean}$ of a patient's lesions was exemplarically used along with the corresponding $SUV_{max}$, lesion size and measured HU. The influence of lesion size, measured HU and liver SUV and liver HU on lesion SUV, was examined with multiple regression analysis. The ratio $HU_{lesion}/HU_{liver}$ was also tested (simple regression analysis) to roughly account for interindividual differences in dynamics of contrast enhancement. Results are given in Table 3.

In contrast to intraindividual analysis, with multiple regression analysis, there was no correlation between lesion size and lesion $SUV_{mean}$ (see Fig. 6). Note the great variability of median lesion $SUV_{mean}$ between individuals ($n$=10) by a factor ~5. For $SUV_{liver}$ and $HU_{liver}$, there was a borderline significant relationship with median lesion $SUV_{mean}$ in terms of a positive and negative correlation, respectively. However, when restricting the analysis to liver lesions only, these borderline significances were clearly lost ($p \geq 0.4$, each) pointing to a missing influence of these parameters on lesion SUV. As with intraindividual analysis, for lesion HU (and $HU_{lesion}/HU_{liver}$), there was no significant relationship with lesion $SUV_{mean}$ in any of the analyses. The data were not significantly different when using $SUV_{max}$ instead of $SUV_{mean}$ (not shown in detail).

**Table 2** Measured SUVs are significantly smaller in small lesions; measured HUs did not differ between small and large lesions

| | Lesions <1 cm | Lesions >2.5 cm | $p$ |
|---|---|---|---|
| $n$ | 32 | 17 | |
| $SUV_{mean}$ | 14.0±5.9 | 38.5±12.5 | <0.0001 |
| $SUV_{max}$ | 19.3±8.9 | 51.6±16.5 | <0.0001 |
| HU | 97.7±15.5 | 94.4±16.5 | 0.5 |

## Discussion

This PET/CT study investigated the intra- and interindividual variability of somatostatin receptor positive tumour lesions regarding the uptake of Gluc-Lys-[$^{18}$F]FP-TOCA. Tracer uptake was examined with respect to key parameters of morphological imaging, namely, lesion size and measured hounsfield units (HUs) at the arterial phase of contrast-enhanced CT scanning. A great variability in tracer uptake was seen both, intra- and interindividually. *Intra*individual variability, to a great degree, appears to be due to partial volume effects. However, substantial intraindividual variability is left unexplained as also larger lesions, namely, greater than 3 cm (2.5 cm), varied by a factor ~2 (~3) in uptake. *Inter*individual variability in tracer uptake was not significantly correlated with lesion size. Additional factors such as different sstr expression in tumour lesions must be postulated to explain interindividual and also residual intraindividual variability in tracer uptake. Measured HUs did not correlate with tracer uptake neither intraindividually nor interindividually. Of note, PET showed substantially more lesions than CT (+18%).

### Correlation with size

Tracer uptake in different lesions *intra*individually varied from 20 to 100% (related to the intraindividual lesion with maximum uptake). Variability in tracer uptake of intraindividual lesions could be fitted with good accordance with a sigmoid function of lesion size (see Fig. 2). This

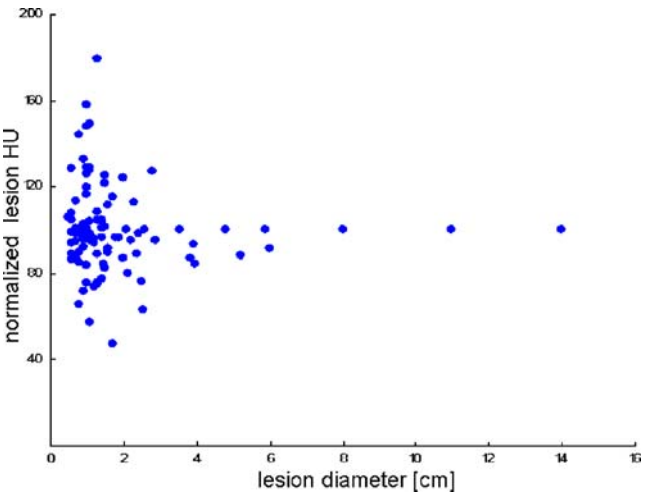


**Fig. 3** No correlation between lesion size and lesion HU after nivellation of interindividual differences in lesion HUs by setting the intraindividual lesion with maximum HU to 100% (precondition: lesion size ≥2 cm)

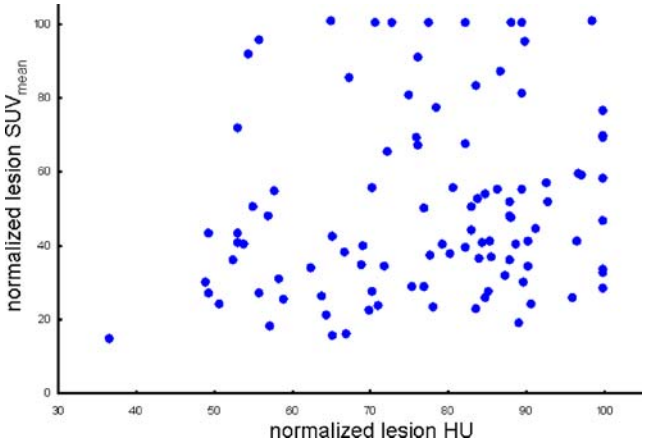


**Fig. 4** No correlation between lesion HU and lesion SUV after nivellation of interindividual differences in lesion HUs and SUVs

**Table 3** Interindividual analysis for potential determinants of lesion $SUV_{mean}$

| | $r^2$ | Coefficient | $p$ |
|---|---|---|---|
| Overall | 0.75 | (Intercept 54) | 0.09 |
| Multiple regression analysis | | | |
| Lesion size | | 8.4 | 0.11 |
| Lesion HU | | 0.03 | 0.90 |
| Liver SUV | | 8.2 | 0.03* |
| Liver HU | | −1.2 | 0.03* |
| Simple regression analysis | | | |
| $HU_{lesion}/HU_{liver}$ | 0.00 | 3.9 | 0.90 |

Overall, no significant correlation was found.
*Not significant when entered single or with each other into regression analysis.

function is characterised by a low plateau as the initial portion (marking approximately the background level of tracer uptake below which tracer uptake in very small lesions cannot fall), a quasi-linear curve as the midportion and a plateau as the terminal portion (starting at ~2.5 to 3 cm lesion size). A sigmoid type of correlation with lesion size is typical of partial volume effects.

As discussed by Brix et al. [15], the degree of partial volume effects is mainly based on, first, spatial resolution of the system, second, lesion size and third, ratio between tracer uptake of the lesion and background. Using a PET system with roughly 5 mm spatial resolution (comparable to the system of this study), those authors set up recovery coefficients for cylindrical phantoms applying different target/background tracer ratios and different diameters of the phantoms. Table 4 opposes our results (according to equation 3) to the recovery coefficients of Brix et al. as interpolated at a target/background ratio of 4.7, which was the mean observed ratio $SUV_{lesion \geq 2\ cm}/SUV_{liver}$ in our study.

On average, our recovery of maximum lesion uptake was slighty lower than the recovery coefficients found by Brix et al. The main differences between our study and that of Brix et al. were, first, that our lesions and ROIs were both approximately spherical in shape rather than cylindrical and circular, respectively. This leads to more pronounced partial volume effects arising from three dimensions instead of two. Second, we conducted a clinical study where voluntary and involuntary patient movements give rise to an additional blurring, which further reduces the signal of lesions and thus the recovery of true activity. Differences in ROI analysis and reconstruction methods may be further limitations to comparability (however, no differences between usage of $SUV_{mean}$ and $SUV_{max}$ was found in this study). Taking into account these differences, we suggest partial volume effects as the main determinant for the intraindividual relationship between SUV and lesion size.

Whereas the general trend towards higher SUVs in bigger lesions is well explicable by partial volume effects, the scatter of the results around this trend is more difficult to explain. At a lesion size above 2.5 cm no major partial volume effects are to be expected. When considering a

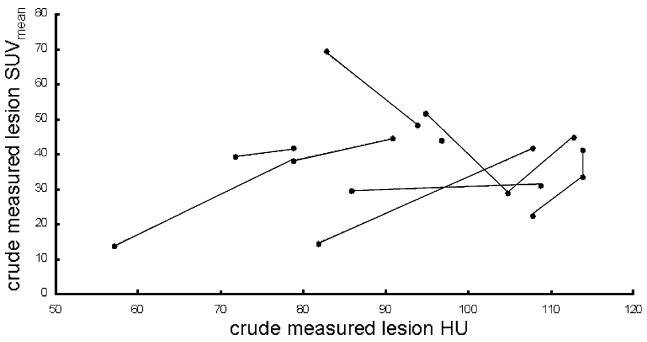


**Fig. 5** No correlation between crude measured HUs and SUVs in lesions >2.5 cm. *Lines* connect lesions belonging to individual patients. No recognizable pattern for an overall upslope or downslope tendency in individual patients (3 upslope, 2 downslope/complex, 2 rather horizontal)

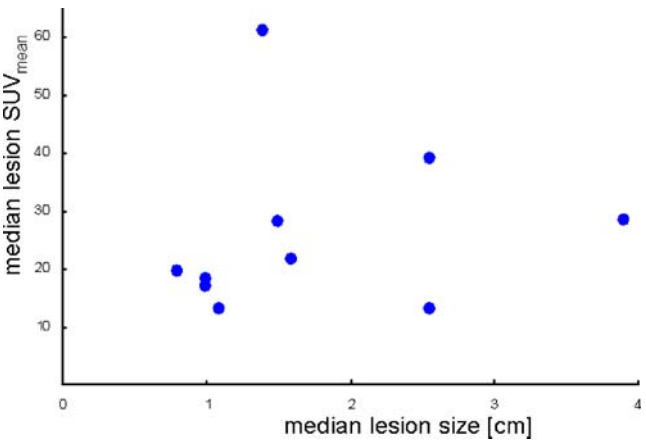


**Fig. 6** No significant interindividual correlation between lesion size and lesion SUV. The respective median of all intraindividual lesions was used as a representative for each individual

**Table 4** Comparison of recovery coefficients from Brix et al. with results of this study

| Diameter (cm) | Percent maximum uptake | Recovery coefficients (%) |
|---|---|---|
| Target (lesion) | This study | Brix et al. |
| 0.8 | 22 | 28 |
| 1.3 | 47 | 66 |
| 1.6 | 64 | 76 |
| 2.1 | 86 | 89 |

clinical situation with additional blurring of the signal by patient movements one might also plead for a 3-cm criterium for lesion size above which no partial volume effects should occur. However, in lesions ≥3 cm, we observed SUVs down to ~50% that of the lesion with maximum uptake. Sub-analysis of these lesions revealed no obvious physical reason such as an extraordinarily high-ratio lesion/background.

Also, tumour necrosis could be ruled out as a possible confounder as tumour necrosis occurred in only 5/114 lesions and all measurements were done in the perfused rim/tumour maximum only. As uptake of Gluc-Lys-([$^{18}$F]FP)-TOCA mainly reflects the density of sstr2 on the cell surface, we assume differences in sstr2 expression to explain residual intraindividual variability in lesion SUVs. However, these deliberations are based on the general concept of tracer–receptor interaction rather than objective results. To date, no study, to our knowledge, has directly compared sstr density on neuroendocrine tumours and uptake of radiolabelled sst analogs.

With regard to *inter*individual variability in lesion SUVs, no significant relationship with lesion size was found. However, partial volume effects inevitably occur not only intraindividually but also interindividually. Therefore, it must be assumed that the trend driven by partial volume effects was not detected only because of a too low number of individuals ($n$=10). Or, in other words, this underlying trend was overshadowed by the great variability of lesion SUVs around this trend. This hypothesis would be in line with the above assumption of lesion differences in sstr2 expression: such differences would then cause scattered results not only intraindividually but also and understandably even more pronounced interindividually.

### Correlation with measured HU

The increase in measured lesion HUs at the arterial phase after administration of contrast medium first of all stands for the perfusion of a lesion reflecting the intravascular content of contrast medium. Second, as some (tumour) vessels may be porous, some contrast medium may have already entered the interstitium at this phase. One may assume a positive correlation between measured lesion HUs on arterial phase CT and lesion SUV on PET as both intravascular and interstitial delivery may coact with regard to the supply of Gluc-Lys-([$^{18}$F]FP)-TOCA to tumour cells.

However, neither intraindividual nor interindividual analysis revealed any recognizable relationship between measured HUs and lesion SUVs. For interindividual analysis there are multiple methodical limitations to consider such as the dependence of the measured HUs on the amount and rate of administered contrast medium, individual parameters of blood circulation and of tissue density and composition. However, these factors do not confound intraindividual analysis. This leads to the conclusion that the contribution of perfusion in determining overall uptake of Gluc-Lys-[$^{18}$F]FP-TOCA in lesions is negligible. Other factors, such as presumably the degree of sstr2 expression in lesions, appear to surpass the role of perfusion by far.

## Conclusion

The only relationship found in this study, between tracer uptake and key parameters of morphological imaging, was an intraindividual positive correlation between lesion SUV and lesion size. Manner and magnitude of this correlation suggest partial volume effects as the major determinant. However, to explain residual intraindividual scatter in lesion uptake—most of all in bigger lesions—as well as interindividual scatter, biological variability must be postulated, e.g. a different sstr2 expression on the surface of tumour cells.

In terms of radionuclide therapy with radiolabelled somatostatin analogues, any variability in lesion uptake may hamper the therapeutic success as therapy must be tailored to and may be limited by the lesions with the least uptake. This study suggests that lesions below 2.5 to 3 cm in diameter should be used with caution for representative dose calculations because of interfering partial volume effects. Above this size, when using the lesion with the greatest uptake for dose calculation, one should bear in mind that—presumably for biological reasons—uptake in some lesions may go down to as low as one-half (or even third) that of the maximum.

## References

1. Meisetschlager G, Poethko T, Stahl A, Wolf I, Scheidhauer K, Schottelius M, et al. Gluc-Lys([18F]FP)-TOCA PET in patients with SSTR-positive tumors: biodistribution and diagnostic evaluation compared with [111In]DTPA-octreotide. J Nucl Med 2006;47:566–73.
2. Schottelius M, Poethko T, Herz M, Reubi JC, Kessler H, Schwaiger M, et al. First (18)F-labeled tracer suitable for routine

clinical imaging of sst receptor-expressing tumors using positron emission tomography. Clin Cancer Res 2004;10:3593–606.
3. Wester HJ, Schottelius M, Scheidhauer K, Meisetschlager G, Herz M, Rau FC, et al. PET imaging of somatostatin receptors: design, synthesis and preclinical evaluation of a novel (18)F-labelled, carbohydrated analogue of octreotide. Eur J Nucl Med Mol Imaging 2003;30:117–22.
4. Reubi JC, Schar JC, Waser B, Wenger S, Heppeler A, Schmitt JS, et al. Affinity profiles for human somatostatin receptor subtypes SST1-SST5 of somatostatin radiotracers selected for scintigraphic and radiotherapeutic use. Eur J Nucl Med 2000;27:273–82.
5. Stahl A, Meisetschlager G, Schottelius M, Bruus-Jensen K, Wolf I, Scheidhauer K, et al. [(123)I]Mtr-TOCA, a radioiodinated and carbohydrated analogue of octreotide: scintigraphic comparison with [(111)In]octreotide. Eur J Nucl Med Mol Imaging 2006;33:45–52.
6. Wester HJ, Schottelius M, Scheidhauer K, Reubi JC, Wolf I, Schwaiger M. Comparison of radioiodinated TOC, TOCA and Mtr-TOCA: the effect of carbohydration on the pharmacokinetics. Eur J Nucl Med Mol Imaging 2002;29:28–38.
7. Antunes P, Ginj M, Zhang H, Waser B, Baum RP, Reubi JC, et al. Are radiogallium-labelled DOTA-conjugated somatostatin analogues superior to those labelled with other radiometals? Eur J Nucl Med Mol Imaging 2007;34:982–93.
8. Koenig JA, Kaur R, Dodgeon I, Edwardson JM, Humphrey PP. Fates of endocytosed somatostatin sst2 receptors and associated agonists. Biochem J 1998;336 (Pt 2):291–98.
9. Bodei L, Cremonesi M, Zoboli S, Grana C, Bartolomei M, Rocca P, et al. Receptor-mediated radionuclide therapy with 90Y-DOTA-TOC in association with amino acid infusion: a phase I study. Eur J Nucl Med Mol Imaging 2003;30:207–16.
10. Cremonesi M, Ferrari M, Zoboli S, Chinol M, Stabin MG, Orsi F, et al. Biokinetics and dosimetry in patients administered with (111)In-DOTA-Tyr(3)-octreotide: implications for internal radiotherapy with (90)Y-DOTATOC. Eur J Nucl Med 1999;26:877–86.
11. Krenning EP, Kwekkeboom DJ, Valkema R, Pauwels S, Kvols LK, De Jong M. Peptide receptor radionuclide therapy. Ann N Y Acad Sci 2004;1014:234–45.
12. Waldherr C, Pless M, Maecke HR, Haldemann A, Mueller-Brand J. The clinical value of [90Y-DOTA]-D-Phe1-Tyr3-octreotide (90Y-DOTATOC) in the treatment of neuroendocrine tumours: a clinical phase II study. Ann Oncol 2001;12:941–45.
13. Waldherr C, Pless M, Maecke HR, Schumacher T, Crazzolara A, Nitzsche EU, et al. Tumor response and clinical benefit in neuroendocrine tumors after 7.4 GBq (90)Y-DOTATOC. J Nucl Med 2002;43:610–6.
14. Cremonesi M, Ferrari M, Chinol M, Bartolomei M, Stabin MG, Sacco E, et al. Dosimetry in radionuclide therapies with 90Y-conjugates: the IEO experience. Q J Nucl Med 2000;44:325–32.
15. Brix G, Bellemann ME, Hauser H, Doll J. [Recovery coefficients for the quantification of the arterial input functions from dynamic PET measurements: experimental and theoretical determination]. Nuklearmedizin 2002;41:184–90.